

# Measured Effectiveness of Deep N-well Substrate Isolation in a 65nm Pixel Readout Chip Prototype

Peilian Liu<sup>1</sup>, Maurice Garcia-Sciveres, Timon Heim, Dario Gnani

*Physics Division, Lawrence Berkeley National Laboratory, Berkeley, CA 94720, USA*

---

## Abstract

The same charge sensitive preamplifier and discriminator circuit with different isolation strategies has been tested to compare the isolation of both analog and digital circuits from the substrate of a 65 nm bulk CMOS process to the isolation of only digital circuits, tying analog ground locally to the substrate. This study will show that the circuit with analog on the substrate and digital in deep N-well has better noise isolation between analog and digital.

*Keywords:* Pixel Readout Chip, Substrate Isolation

---

## 1. Introduction

A significant concern for mixed signal circuits, and for detector front end Application Specific Integrated Circuits (ASICs) in particular, is the isolation of sensitive analog nodes from digital activity. Bulk CMOS technologies typically offer deep implants that can be used to electrically isolate individual transistors or full circuit blocks from the substrate. How to handle the substrate and what isolation strategy to use can depend on the particular CMOS process, but can be informed by general guidelines. It is normally not practical to prototype alternative isolation strategies in order to select one, as it requires to duplicate the same ASIC with alternative isolation in order to compare the two.

For this note we take advantage of a rare opportunity to prototype and test the same complex circuit with different isolation strategies, and compare

---

<sup>1</sup>Corresponding author, email: peilianliu@lbl.gov

the results. We compare the isolation of both analog and digital circuits from the substrate of a 65nm bulk CMOS process (effectively leaving the substrate as a buffer with no electrical function) to the isolation of only digital circuits, tying analog ground locally to the substrate. We refer to the former as double isolation and to the latter as digital isolation. A pixel readout matrix demonstrator ASIC, called FE65-P2 [1], was fabricated twice, once with double isolation (original design from [2]) and once with digital isolation, by simply removing the deep n-well layer from the analog front end “islands” in pixel matrix with no other changes.

The FE65-P2 contains a matrix of 64 by 64 pixels on  $50\mu\text{m}$  by  $50\mu\text{m}$  pitch. Every pixel has a dedicated analog front end, consisting of a charge integrator, followed by a single ended to differential second stage feeding a differential comparator, shown in Fig. 1. The pixel threshold is controlled by

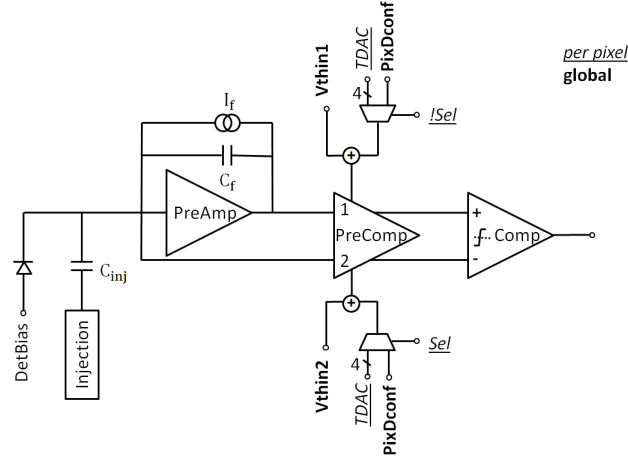


Figure 1: Schematic diagram of a pixel analog front end.

two global, internal 8-bit DACs ( $V_{thin1}$  and  $V_{thin2}$ ). All pixels receive the same global threshold voltages, but each pixel’s effective threshold will occur at a different DAC value due to natural mismatch. The FE65-P2 includes a 5-bit trim DAC (TDAC) in each pixel to compensate for this mismatch.

The front ends are laid out in compact groups of four pixels or quads (also called analog islands) sharing power and bias distribution, as shown in Fig. 2. The analog islands are surrounded on all sides by synthesized logic, isolated from the substrate by a deep N-well. Each island is in its own, separate deep N-well in the double isolated chip, or directly on the substrate in the digital

isolated chip. Configuration bits for front end tuning and function selection are stored in the synthesized digital logic and supplied to each front end quad as static CMOS levels.

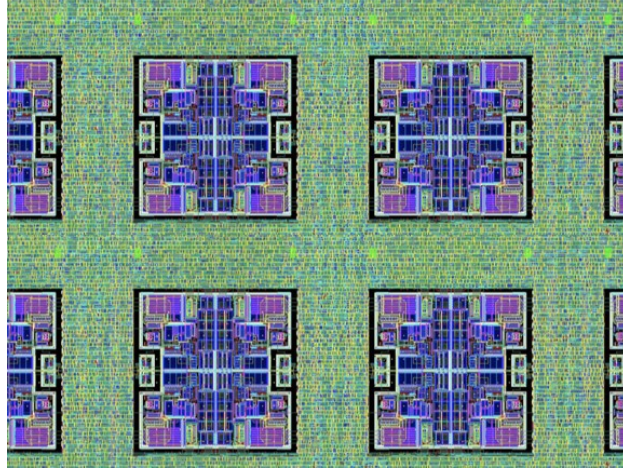


Figure 2: Layout detail showing an analog quad island surrounded by synthesized logic.

We measured two each double isolated and digital isolated FE65-P2 chips. Each bare die was mounted on its own passive test card, which could be connected to an active interface board to power, computer and instruments. A useful FE65-P2 feature for this study is the ability to disable all digital activity in the pixel matrix and still have access to the discriminated analog pixel outputs, one at a time, via a dedicated global OR hit output. We refer to this mode as “digital off”. This permits observing an ideal critical threshold baseline for one pixel at a time.

## 2. Method

All measurements were done with the same interface card and identical setup and control software, so that the only difference between the double isolated and digital isolated chip measurements was the chip itself. We take as a figure of merit of the isolation performance the observed single pixel noise increase caused by selected aggressor signals applied to the digital domain only. Thus any observed noise increase from aggressor off to aggressor on is the result of these aggressors coupling from the digital to the analog domain.

The intrinsic analog front end noise ( $\sigma_A$ ) is obtained with digital off by fitting an S-curve to the response counts vs. injected charge of each pixel

discriminator output, as illustrated in Fig. 3 (a). Fig. 3 (b) shows the width of S-curve ( $\sigma_A$ ) obtained in each pixel of all measured chips. The difference of the noise distribution between two different chips of the same type is comparable with the dispersion observed with ten FE-I4B wafers in Ref. [3]. The act of injecting charge can potentially introduce a small bias, but final result, which is a relative measurement, is insensitive to the absolute value of noise measured here.

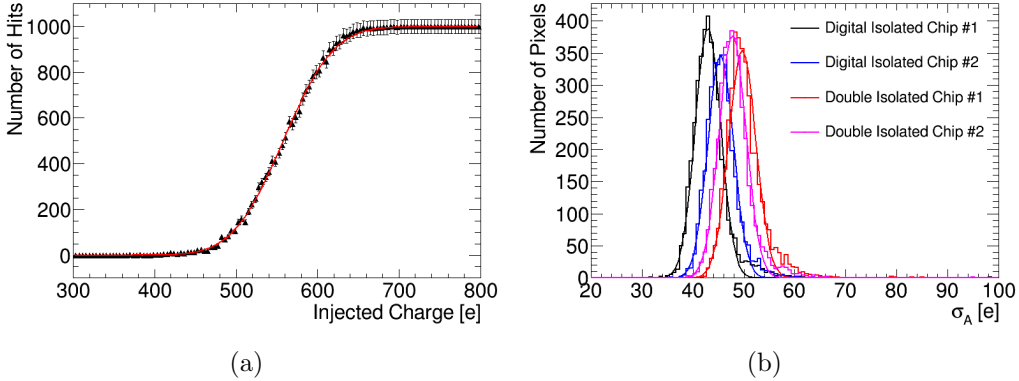


Figure 3: (a) Illustration of S-curve obtained by counting number of hits with changing the injected charge. (b) Intrinsic analog front end noise obtained with digital off in each pixel of all measured chips.

To measure noise differences in a more sensitive and unbiased way, we do not use charge injection and S-curve reconstruction, but instead measure pixel noise occupancy (NOCC) as a function of threshold. The NOCC is defined as the number of noise hits observed in one pixel in one second interval, which is the same as the mean pixel firing frequency. Thus a NOCC of  $10^{-1}$  means that a pixel free-fires at an average rate of 0.1 Hz. At a high value of threshold there will be zero NOCC. As the threshold is gradually decreased, the NOCC begins to rise exponentially. We plot NOCC vs. threshold on a log scale and find the intercept of a line fit (on the log scale) with a “floor” occupancy of 0.1. We call this intercept the critical threshold.

The critical threshold is a very sensitive measure of noise. Assuming that noise is Gaussian and that at zero threshold the NOCC is of order  $10^6$ , the critical threshold of 0.1 is about  $5\sigma$  away from zero. Therefore, if we observe the critical threshold shift by an amount  $x$  in response to an aggressor signal,

this represents a change in noise  $\sigma$  of  $x/5$ . Thus we can detect smaller noise changes than possible by fitting an S-curve. Additionally, because the NOCC measurement does not use any charge injection, it does not introduce perturbations that can bias the measurement.

We use two ways to measure NOCC: (a) direct transition frequency measurement of the hit output of a single pixel at a time, using an edge triggered frequency counter, and (b) counting recorded hits using the normal triggered readout of the pixel matrix, by enabling a large number of pixels at a time and repeatedly triggering chip readout.

### 3. Single pixel measurements without noise injection: method (a)

Method (a) makes use of the dedicated global OR hit output. With the clock disabled the chip is effectively a pure analog circuit and any noise observed is the intrinsic front end noise. When the clock is enabled and the digital circuitry is active, the possibility arises (due to less than perfect isolation) for digital noise to couple to the analog domain. This would show up as an increase in the measured noise.

Vthin2 is kept to be 30 in all measurements through this paper. The trim threshold voltage in the pixel being studied is always set to the lowest value, to get reasonable noise occupancy. The trim threshold voltage of all other pixels are set to the highest value, in order to decrease the noise from other pixels. The threshold is changed by only changing Vthin1. Fig. 4 shows single pixel NOCC vs. Vthin1 with digital off or on, for a few selected pixels on one of our tested chips, along with straight line fits intersecting the 0.1 Hz horizontal line to extract the intercept which is called critical Vthin1.

Fig. 5 illustrates the threshold in electrons as a function of Vthin1. The threshold vs. Vthin1 distribution is fit with a linear function in the threshold range of 600 [e] to 1000 [e]. Critical threshold is calculated with critical Vthin1 and the relationship between threshold and Vthin1.

Fig. 6 shows the change of critical threshold (referred as  $\delta$ [e]) when digital is on relative to digital off, which indicates the aggressor effect of clocking the chip logic relative to the clock off baseline.

Based on the intrinsic front end noise width ( $\sigma_A$ ) and the width of the noise which spreads from digital to analog ( $\sigma_D$ ), the total noise obtained in analog with digital on would be  $\sigma_{A \otimes D} = \sqrt{\sigma_A^2 + \sigma_D^2}$ . If we assume the critical threshold is at the  $5\sigma$  of the noise distribution, then we have  $\delta = 5 \cdot \sigma_{A \otimes D} - 5 \cdot \sigma_A$ . Therefore,  $\sigma_D$  could be calculated with  $\sqrt{(\delta/5 + \sigma_A)^2 - \sigma_A^2}$ .

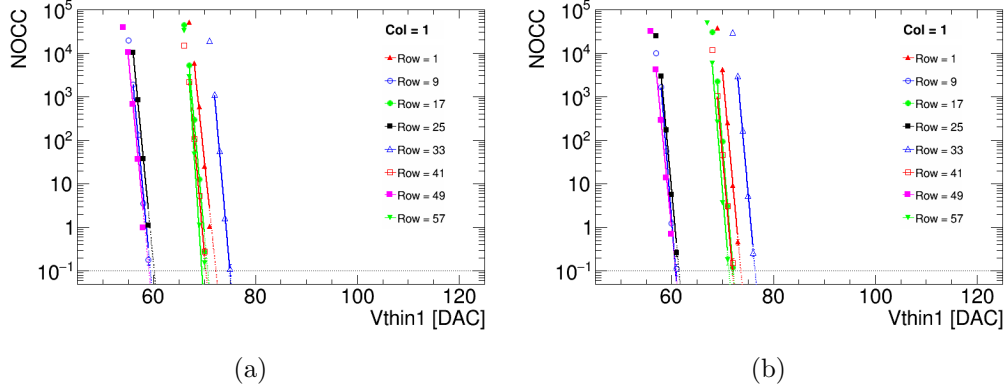


Figure 4: Single pixel NOCC vs. threshold data for a few selected pixels with digital off (a) or on (b) in the first pixel column of the double isolated chip, obtained by counting recorded hits pixel by pixel using the global OR hit output of the discriminated analog.

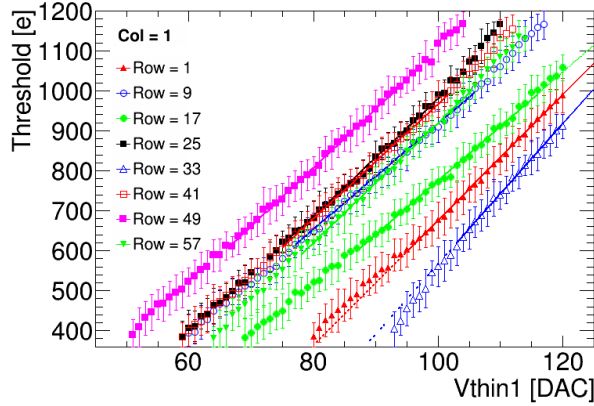


Figure 5: Threshold vs.  $V_{thin1}$  for a few selected pixels in one of the double isolated chips.

Fig. 7 shows the aggressor effect of pixel readout measured using method (a). While many pixels are enabled and read out, only one pixel at a time can be measured. The result is shown for a few measured pixels.  $\sigma_D$  distributions shown in Fig. 7 imply the digital isolation is better. However we do not control the characteristics of the noise injected by digital activity. To get some kind of noise transfer function from digital to analog we need to directly inject noise into the digital domain.

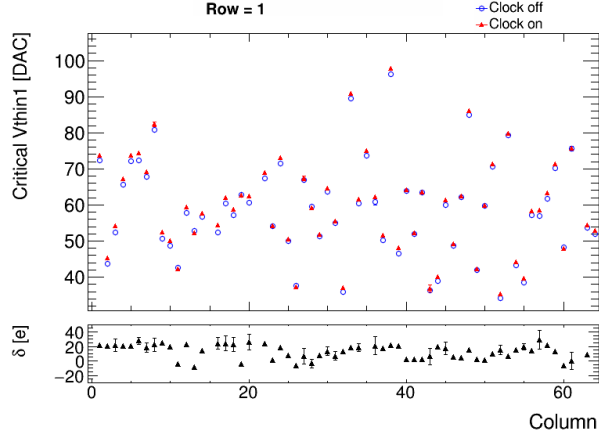


Figure 6: The change of critical threshold when digital is on relative to digital off in the pixels of the first row of the double isolated chip.

#### 4. Pixel matrix measurements: method (b)

Method (b) uses the normal triggered readout of the pixel matrix by enabling a large number of pixels at a time. The digital is always on. It exploits the FE65-P2 feature of power monitoring pads at the chip top (while the power is supplied from the chip bottom). Thus, in FE65-P2 we are able to run an externally controlled current through the digital power distribution network, independently from the chip current consumption. This current is our noise injection method. The injection method is shown schematically in Fig. 8. The digital power supply at the chip bottom (VDDD) is kept at 1.2 V as usual, while an A/C signal to the monitoring pad at the chip top (VDDD\_TOP) is used to draw an A/C across the external load resistor. The highest voltage of the A/C signal (with frequency  $f$ ) is always 1.2 V, while the lowest voltage changes among different measurements to produce different amplitude of current ( $I_{\text{inject}}$ ).

The first measurement is based on square wave, the frequency of which is 1 MHz. The injected current amplitude was 4.8 mA (this can be compared with the internal digital consumption of 23 mA). Fig. 9 shows single pixel NOCC vs. threshold data for a few selected pixels on one of our tested chips, along with straight line fits intersecting the 0.1 Hz horizontal line to extract the critical threshold. The critical threshold increased significantly due to the current changes in pixel columns. The change of critical threshold after injecting current is  $\delta = 5 \cdot \sigma_A \otimes D' - 5 \cdot \sigma_A \otimes D$ .  $\sigma_A \otimes D'$  ( $\sigma_A \otimes D$ ) is the

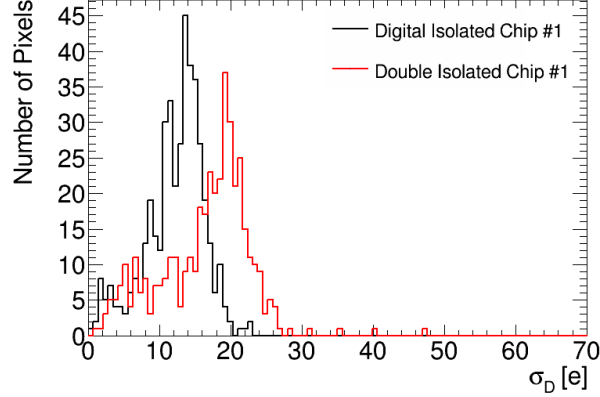


Figure 7: Intrinsic  $\sigma_D$  obtained without noise injection using method (a).

width of the noise observed in analog with (without) injecting current when digital is on.  $\sigma_{A \otimes D}$  is obtained with digital on by fitting an S-curve to the response counts vs. injected charge of each pixel discriminator output.  $\sigma_{A \otimes D'}$  is calculated with  $\delta/5 + \sigma_{A \otimes D}$ . Therefore, the width of the noise which spreads from digital to analog with injecting current and digital on,  $\sigma_{D'}$ , could be calculated with  $\sqrt{\sigma_{A \otimes D'}^2 - \sigma_A^2}$ .

Fig. 10 shows the  $\sigma_{D'}$  distribution when 4.8 mA current (1 MHz square wave) is injected to digital. This measurement with method (b) also indicates the digital isolation is better than double isolation.

To study the frequency dependence of the noise coupling we use a sine wave instead of a square wave. Higher amplitude of waveform induces more noise. The double isolated chips are measured using a sine wave with 1.2 mA current injected to digital. The digital isolated chips are measured using a sine wave with 2.4 mA current injected to digital. To easily compare two isolation, the change of critical threshold is divided by the amplitude of the injected current. When the amplitude of the injected current is too high, some pixels could not work normally due to the high noise spreads from digital to noise. This is why lower amplitude current is injected in double isolated chips. Fig. 11 shows the average of  $\sigma_{D'}$  per mA among the measured pixels in each chip. The uncertainty of each measurement point is the root mean square of the  $\sigma_{D'}$  distribution. Relative to double isolated chips, the  $\sigma_{D'}$  vs. frequency in digital isolated chips is more flat and lower.



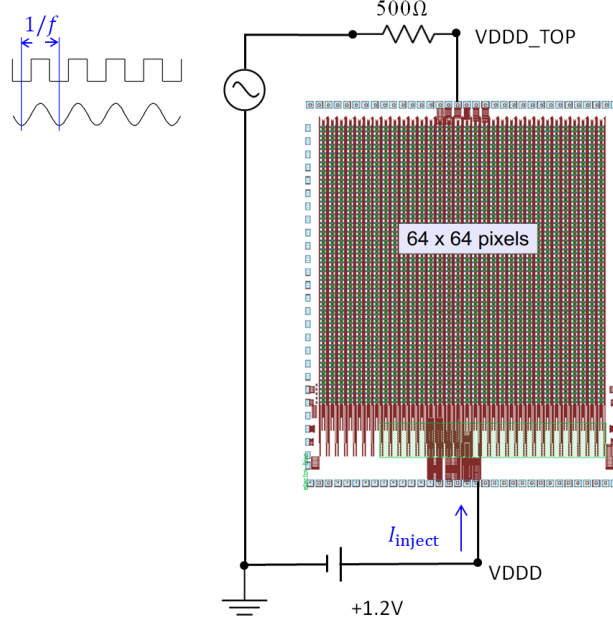


Figure 8: Schematic of current injection ( $I_{\text{inject}}$ ) to digital. The digital power supply to VDDD is kept at 1.2 V. The highest voltage of the A/C signal (with frequency  $f$ ) to VDDD\_TOP is always 1.2 V, while the lowest voltage changes among different measurements.

## 5. Conclusion

Two methods have been applied to measure the isolation between analog and digital. Our measurements indicate that the digital isolation is better than double isolation. Nevertheless, both isolation strategies perform well for normal operation (Fig. 7): attempts to inject voltage noise on the digital supply failed to produce any measurable effect, and only the current injection (method (b)) succeeded. The reason why digital isolation is better than double isolation might be noise is coupling through metal stack rather than substrate. In this case the double isolation has a higher impedance analog ground that is easier to shake by noise coming from the metal stack.

## 6. Acknowledgements

This work was supported by the U.S. Department of Energy, Office of Science under contract DE-AC02-05CH11231. The chip fabrication was supported by the RD53 Collaboration.

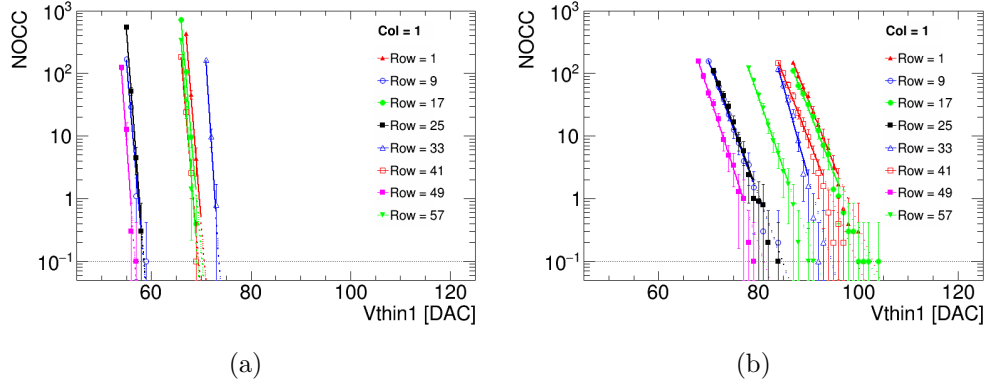


Figure 9: Single pixel NOCC vs. threshold data for selected pixels before (a) and after (b) injecting 4.8mA current by an square wave with  $f = 1$  MHz, obtained by counting recorded hits using the normal triggered readout of the pixel matrix.

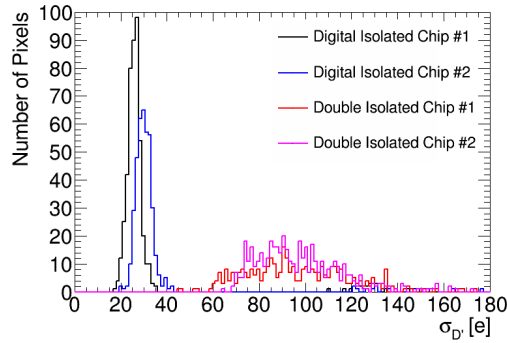


Figure 10:  $\sigma_{D'}$  obtained by injecting 4.8mA current (1MHz square wave) to digital.

## 7. References

### References

- [1] M Garcia-Sciveres et al., Results of FE65-P2 Pixel Readout Test Chip for High Luminosity LHC upgrades, Proc. 38th Int. Conf. on High Energy Physics (2016) p272.
- [2] The RD53 collaboration, Recent progress of RD53 Collaboration towards next generation Pixel Read-Out Chip for HL-LHC, JINST 11 (2016) C12058.

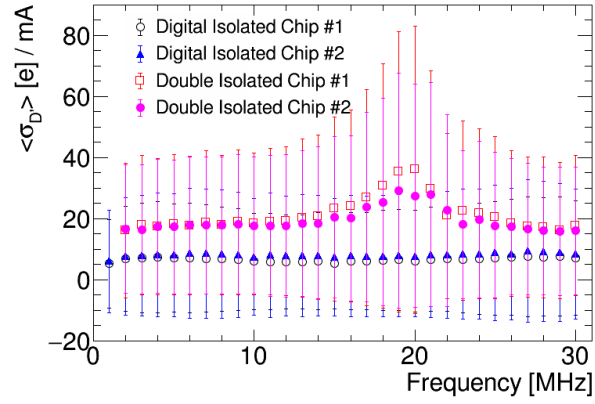


Figure 11: Average of  $\sigma_D$  per mA vs the injected current frequency of sine wave in all of measured chips.

- [3] M Backhaus, Characterization of the FE-I4B pixel readout chip production run for the ATLAS Insertable B-layer upgrade, JINST 8 (2013) C03013.